BioSystems 199 (2021) 104310

Contents lists available at ScienceDirect

BioSystems

journal homepage: www.elsevier.com/locate/biosystems

Dynamical diversity of mitochondrial BK channels located in different cell types

Agata Wawrzkiewicz-Jałowiecka [a,*], Paulina Trybek [b], Łukasz Machura [c], Piotr Bednarczyk [d]

[a] Department of Physical Chemistry and Technology of Polymers, Faculty of Chemistry, Silesian University of Technology, Gliwice, 44-100, Poland
[b] Faculty of Science and Technology, University of Silesia in Katowice, Chorzow, 41-500, Poland
[c] Institute of Physics, University of Silesia in Katowice, Katowice, 40-007, Poland
[d] Institute of Biology, Department of Physics and Biophysics, Warsaw University of Life Sciences - SGGW, Warszawa, 02-787, Poland

ARTICLE INFO

Keywords:
MitoBK channels
βsubunits
Hurst exponent by DFA method
Multiscale entropy MSE
Focus-based multifractal analysis MFDFA
Gating dynamics

ABSTRACT

Mitochondrial large-conductance voltage- and Ca^{2+}-activated potassium channels (mitoBK) exhibit substantial similarities in their physiology regardless of the channel's location. Nevertheless, depending on the cell type, composition of membranes can vary, and mitoBK channels can be expressed in different splice variants as well as they can be co-assembled with different types of auxiliary β subunits. These factors can modulate their voltage- and Ca^{2+}-sensitivity, and single-channel current kinetics. It is still an open question to what extent the mentioned factors can affect the complexity of the conformational dynamics of the mitoBK channel gating. In this work the dynamical diversity of mitoBK channels from different cell types was unraveled by the use of nonlinear methods of analysis: multifractal detrended fluctuation analysis (MFDFA) and multiscale entropy (MSE). These techniques were applied to the experimental series of single channel currents. It turns out that the differences in the mitoBK expression systems influence gating machinery by changing the scheme of switching between the stable channel conformations, and affecting the average number of available channel conformations (this effect is visible for mitoBK channels in glioblastoma cells). The obtained results suggest also that a pathological dynamics can be represented by signals of relatively low complexity (low MSE of the mitoBK channel gating in glioblastoma).

1. Introduction

Mitochondria are intracellular organelles which play a key role in several cellular processes: respiration, regulation of cell signaling, differentiation, cell growth, apoptosis, cell cycle or steroidogenesis (Wang, 2001; Duchen, 2000; Halestrap, 1994; Papadopoulos and Miller, 2012; Kowaltowski et al., 2009). Mitochondria are shaped by two membranes: the outer and the inner membrane, which delimit two areas, i.e. the intermembrane space and the mitochondrial matrix. The inner mitochondrial membrane, where the respiratory chain protein complexes are embedded, greatly contributes to the mitochondrial metabolism and ATP synthesis (via oxidative phosphorylation). The efficiency of these processes strongly depends on the activity of ion channels present in the inner mitochondrial membrane (Szabo and Zoratti, 2014).

The large-conductance voltage- and Ca^{2+}-activated potassium channels were described in inner mitochondrial membranes (mitoBK) in a number of mammalian cell lines (glioblastoma, cardiomyocytes, endothelial cells, fibroblasts etc. Balderas et al., 2015; Szabo and Zoratti, 2014; Bednarczyk et al., 2013a; Kicinska et al., 2016; Bednarczyk et al., 2013b). In different locations the mitoBK channels exhibit substantial similarities in their physiology, like: single channel conductance (ca. 300 pS), sensitivity to membrane depolarization or Ca^{2+} concentration, underlying blockade by toxins: charybdotoxin (ChTx) and iberiotoxin (IbTx). Nevertheless, some differences in their functioning can be detected for different channel's isoforms. Depending on the splice variation of mitoBK channel or its association with auxiliary subunits (β (1–4) and γ (1–4)) gating kinetics as well as the dependence of channel conductance on voltage and Ca^{2+} may significantly differ (at quantitative level).

Auxiliary β subunits are exhibited in different cell types in a tissue-specific manner which renders them meaningful in defining the function of mitoBK channels in different organs (Contreras et al., 2012). For example, the association of mitoBK channel with its auxiliary β1 subunit is essential for maintaining mitochondrial Ca^{2+} homeostasis in cardiac cells (Balderas et al., 2019) (the lack of the regulatory β1 subunit results in reduced mitoBK channel activity which impairs mitochondrial Ca^{2+} handling). What is more, the distribution of a particular

* Corresponding author.
E-mail address: agata.wawrzkiewicz-jalowiecka@polsl.pl (A. Wawrzkiewicz-Jałowiecka).

https://doi.org/10.1016/j.biosystems.2020.104310
Received 27 August 2020; Received in revised form 20 November 2020; Accepted 20 November 2020
Available online 25 November 2020

β subunits can differ within the functional parts of an organ, which tunes its healthy functioning. This occurs in case of the β4 subunit distribution throughout the brain (Piwonska et al., 2008). The differences in β4 expression levels in distant regions of brain suggest that the abundance of this subunit can play a regulatory role in maintaining the proper efficiency of the ionic transport through mitochondrial BK channels in neurons (Piwonska et al., 2008).

So far as the differences in channel kinetics, sensitivity to activating factors or pharmacological stimulation for different mitoBK splice variants are reported, the question of similarities and discrepancies in conformational dynamics of a system remains unknown. In Ref. Tao and MacKinnon (2019) the authors determined long-awaited atomistic cryo-EM structures for the full-length human BK channel in complex with β4 subunit in high and low Ca^{2+} concentration regimes. This report throws a new light for molecular mechanisms of ionic conductance and the coupling between ligand- or voltage sensors, auxiliary subunits and the channel pore. The analysis of the stable BK channel structures at high and low Ca^{2+} concentrations showed that identical gating conformations occur in the absence and presence of modulatory β4 subunit. Thus, the authors concluded that the β4 ought to modulate the relative stabilities of 'preexisting' conformations rather than creating new ones during Ca^{2+}-activation of the channel. Nevertheless, the impact of β subunits on voltage-activation, especially at the level of single open-closed fluctuation events, is not fully understood. Since the mitoBK channels are encoded by the same gene as the BK channels in the plasma membrane (Kcnma1) (Singh et al., 2013) one can expect that the β subunits should exert analogical influence on the conformational space of the mitochondrial BK channel protein as on the ones located in a cell membrane.

From this perspective, it is desirable to determine how the different types of regulatory β subunit can affect the complexity of conformational dynamics during gating of mitoBK channel, and how it is represented in a single channel activity. In aim to answer these questions we analyze experimental time series of single mitoBK channel currents obtained by the patch-clamp method from three independent human cell lines: endothelial cells (EA.hy926) (Bednarczyk et al., 2013a), dermal fibroblasts (HDFa) (Kicinska et al., 2016), glioblastoma (astrocytoma, U-87 MG) (Bednarczyk et al., 2013b), where the mitoBK channels are associated with auxiliary β2, β3 and β4 subunits, respectively. The presence of α and appropriate β subunits of the mitoBK channel in analyzed cells mitochondria was confirmed by Western blot analysis (Bednarczyk et al., 2013a; Kicinska et al., 2016; Bednarczyk et al., 2013b), immuno-gold electron microscopy (Bednarczyk et al., 2013b), high-resolution immunofluorescence assays (Bednarczyk et al., 2013b) and polymerase chain reaction analysis (Kicinska et al., 2016; Bednarczyk et al., 2013b), and their functionality was investigated by the use of some known BK channel modulators (Bednarczyk et al., 2013a; Kicinska et al., 2016; Bednarczyk et al., 2013b).

Even if the dominating components of mitoBK-β assemblies are known in analyzed patches, the population of mitochondrial BK channel isoforms as well as the auxiliary subunits in wild-type cells is not fully homogeneous. Thus, the possible diversity in the mitoBK channel dynamics in different cell lines give strong evidence of how the transcription-related channel alterations as well as the differences in lipid composition of membranes from different locations can affect the observable activity of these transport proteins. Nevertheless, based on our performed biophysical experiments (Bednarczyk et al., 2013a; Kicinska et al., 2016; Bednarczyk et al., 2013b) the most striking differences between patches from different cell lines lay in assembling the α subunit of the mitoBK channel with different types of auxiliary β subunits, and possibly discernible composition of mitoBK channel isoforms. It is difficult to discriminate between the impact of these two factors in a reasonable way. Nevertheless we decided to describe in this research the effects observed in real, wild-type systems. From this perspective, all results mentioned in this work refer to the differences occurring within the channels from versatile cell lines where the leading factor in shaping the results are different, tissue-specific types of β subunits. Still, one has to be conscious that there may exist some other factors influencing the results.

The composition of solutions used in our experiments was adjusted to ensure the maximal level of channel activation by Ca^{2+}. The effects of different location of the channels, and particularly tissue-specific types of the co-assembled β subunits on channel gating dynamics were investigated at different levels of membrane depolarization and hyperpolarization. Namely, the experiments were carried out at following levels of the membrane potential: −60 mV, −40 mV, −20 mV, +20 mV, +40 mV, +60 mV.

Conformational diffusion of a channel protein determines the structure of experimental series of single channel currents. Presence and abundance of distinct channel conformations (sufficiently distant structurally and energetically from each other to be discriminated from the other ones) are suspected to affect the complexity of the experimental data. It is possible that some channel conformations, which substantially differ by inner pore geometry, exhibit a very similar conductance. Still, in most cases, notable differences in shape and size of the pore should lead to significantly different conductances. Application of nonlinear methods in the analysis of an experimental signal allows to estimate the changes in the number of channel states which are available from a geometric and energetic point of view at given external conditions (Wawrzkiewicz-Jałowiecka et al., 2018, 2020b), but not only. The investigation of signal complexity can ensure a deep insight in a real character of the considered biosystem, which is regulated by interacting mechanisms that operate across multiple spatial and temporal scales and contain deterministic and stochastic components. A reasonable choice of the parameters characterizing system's complexity allows to extract and describe leading factors that influence the investigated process.

What is more, the complexity of a biological system reflects its ability to adapt and function in an ever-changing environment. The loss in structural richness of an experimental signal may be often associated with the occurrence of a disrupted or even deeply pathological dynamics (Costa et al., 2005). It is well worth mentioning, that in this work we present the results of complexity analysis of channel currents from "healthy" and tumor cell types. Thus, the recognized differences in current characteristics can not only stem from interactions between the channel protein with different β subunits, but also from invalid features of a signal associated with pathological micro-biosystem of a cancer cell.

Therefore, our analysis should help in correlating distinct properties of electrophysiological signal (time series of single mitoBK channel currents) with molecular composition, and consequently, tissue-specific conformational dynamics of mitoBK channel isoforms in a complex with a different β subunits.

In order to describe the dynamical diversity of mitochondrial BK channels the following independent nonlinear methods of analysis were applied to the experimental time series of single channel currents: (i) multifractal detrended fluctuation analysis (MFDFA) and (ii) multiscale entropy (MSE). Because the channel systems need to operate across multiple spatial and temporal scales, and hence their complexity is also multiscaled, all of the chosen methods of analyzes refer to the features of a system manifested over a range of scales.

The analysis of the spectral parameters obtained by the MFDFA method as well as the multiscale entropy is still not common in studies on the ion channel dynamics. Nevertheless, these characteristics do not only describe multiscale characteristics of channel currents' complexity but also can be interpreted in terms of the conformational diffusion during channel gating.

Carrying out a nonlinear analysis of the experimental single channel currents (by the MFDFA and MSE methods), we ought to answer the questions of how different types of mitoBK-β complexes affect the predictability and structural complexity of a signal, its sensitivity

to large or small fluctuations, and eventually, the number of attainable mitoBK channel conformations and the complexity of switching mechanism between. To facilitate the interpretation of the obtained complexity characteristics and to gain better insight in the structure of the analyzed data, a representative single channel current traces as well as the results of a basic kinetic analysis (including the evaluation of the probability density of a functionally open state (conducting) (p_{op}), mean dwell times of conducting and non-conducting states (τ_{op} and τ_{cl}, respectively)) are presented.

2. Material and methods

2.1. Cell culture

In this work we investigated the activity of the mitochondrial mitoBK channels isolated from three independent commercially available cell lines, where the pore-forming α subunits are associated with different β subunits:

- human endothelial cell line (EA.hy926) (Bednarczyk et al., 2013a) (predominantly with β2 subunits),
- human glioblastoma cell line (astrocytoma U-87 MG) (Bednarczyk et al., 2013b) (predominantly with β4),
- primary human dermal fibroblasts (HDFa) (Kicinska et al., 2016) (predominantly with β3).

Cells were cultured as described previously (Kicinska et al., 2016; Bednarczyk et al., 2013a,b). They were grown in DMEM supplemented with 10% fetal bovine serum at 37 °C in a humidified atmosphere with 5% CO_2. The solutions used in cell culture contained additionally: 2 mM L-glutamine, 100 U/ml penicillin, and 100 mg/ml streptomycin in case of glioblastoma, 1% L-glutamine, 2% hypoxanthine hypoxanthine-aminopterin–thymidine, and 1% penicillin–streptomycin in case of endothelium, 2 mM L-glutamine, 100 U/ml penicillin, and 100 mg/ml streptomycin in case of dermal fibroblasts. The cells were fed and reseeded every third–fourth day.

2.2. Mitochondria and mitoplast preparation

The fresh mitochondria and subsequent mitoplasts were prepared by using differential centrifugation and hypotonic swelling, respectively, as previously described (Kicinska et al., 2016; Bednarczyk et al., 2013a,b). Mitoplasts were prepared from the human endothelium, fibroblast and glioblastoma mitochondria by incubation in a hypotonic solution (5 mM HEPES, 100 μM $CaCl_2$, pH 7.2) for approximately 1 min, and then a hypertonic solution (750 mM KCl, 30 mM HEPES, and 100 μM $CaCl_2$, pH 7.2) was subsequently added to restore the isotonicity of the medium. For each/repeating patch-clamp experiment, a fresh mitoplast preparation was used.

2.3. Analysis of BK channel subunit expression and the immunological detection of mitoBK channel proteins in isolated mitochondria

The existence of mitoBK channel with appropriate auxiliary β2, β3 and β4 subunits in investigated patches was confirmed by Western blot analysis (Bednarczyk et al., 2013a; Kicinska et al., 2016; Bednarczyk et al., 2013b), immuno-gold electron microscopy (Bednarczyk et al., 2013b), high-resolution immunofluorescence assays (Bednarczyk et al., 2013b) and/or polymerase chain reaction (Kicinska et al., 2016; Bednarczyk et al., 2013b). All tests gave strong evidences for the presence of appropriate α and β subunits, for details please see Kicinska et al. (2016) and Bednarczyk et al. (2013a,b).

2.4. Patch-clamp experiments

The experiments were carried out in mitoplast-attached single-channel inside-out mode using a pipette of borosilicate glass (Harvard, UK) with a resistance of 10–20 MΩ, which was pulled using a Flaming/Brown puller. The patch-clamp glass pipette was filled with an isotonic solution containing 150 mM KCl, 100 μM $CaCl_2$ (endothelium) or 200 μM $CaCl_2$ (glioblastoma and fibroblasts), and 10 mM HEPES at pH 7.2. The composition of the pipette solution ensured full Ca^{2+}-activation of the investigated mitoBK channels. All patch-clamp measurements were carried out in an air-conditioned room (24 °C). The current was recorded using a patch-clamp amplifier Axopatch 200B. The currents were low-pass filtered at a corner frequency of 1 kHz and sampled at a frequency of 4.00 kHz (at time intervals of 250.00 μs) with Clampex software. Single channel currents were recorded at fixed pipette potentials of: −60, −40, −20, 20, 40, and 60 mV. The ionic current measurement error was $\Delta I = 1{\times}10^{-6}$ pA (determined by the equipment). Each experimental time series comprised $N = 2 \times 10^5$ current values at the applied time resolution of the measurement. At each value of membrane potential we recorded time series of single mitoBK channel currents using 6–11 independent patches for each cell type.

2.5. Event detection for kinetic analysis

The MFDFA and MSE analyses were carried out on a raw experimental data. However, to evaluate the kinetic statistics (p_{op}, τ_{op}, τ_{cl}) one should determine the threshold current (TC) value used to identify transitions between the subsequent conducting and nonconducting states. The TC was evaluated using the procedure given in Ref. Mercik et al. (1999). Briefly, after plotting the ionic current probability density function (PDF) approximated by the nonparametric kernel density estimate with Epanechnikov kernel in the log–log scale, one can observe, that the obtained estimate is a mixture of two unimodal densities, that in broad intervals satisfy power laws. The TC, in relation to which the functionally open and closed states are identified, is indicated as a point of intersection of the power law plots.

2.6. Multifractal Detrended Fluctuation Analysis (MFDFA)

The *MFDFA* technique is an extension of *Detrended Fluctuation Analysis(DFA)* proposed by Peng in 1994 for investigating the correlation in DNA structure (Peng et al., 1994). In this work the modified MFDFA algorithm in the form of *Focus Based MFDFA* was implemented allowing for the most accurate results. For the details about Focus-based multifractal formalism we refer the reader to Refs. Mukli et al. (2015) and Wawrzkiewicz-Jałowiecka et al. (2020b). The basic formula of MFDFA algorithm is briefly presented below

I. *DFA*

The procedure starts with the estimation of signal's profile y_i as the cumulative sum of the series x_i with the subtracted average value $\langle x \rangle$

$$y_i = \sum_{k=1}^{i} [x_k - \langle x \rangle] \tag{1}$$

Next step consists of splitting y_i into n_s equal non-overlapping segments of size s, for which we use powers of two, $s = 2^a, a = 4 \ldots 12$.

According to the original algorithm (Kantelhardt et al., 2002), since the length of the series y_i is often not a multiple of the considered time scale s, a short part at the end of the signal can remain. In order not to disregard this part of the series, the same procedure is carried out starting from the opposite end. Thus, $2n_s$ segments are obtained altogether. Since in this work the FB-MFDFA algorithm was applied (Mukli et al., 2015) we

follow the modified procedure and analyze only scaling obtained at anterograde windowing for (n_s segments).
For all segments of size s, $v = 1, \ldots, n_s$ the local trend $y^p_{v,i}$ is estimated by means of the least-squares fit of order p. In the further step the variance $F^2(s,v)$ as a function of the segment length s is calculated for each segment v.

$$F^2(s,v) \equiv \frac{1}{s}\sum_{i=1}^{s}\left(y^p_{v,i} - y_{v,i}\right)^2. \tag{2}$$

The Hurst exponent H is determined as the slope of the regression line of double-logarithmic dependence, here $\log F(s) \propto H \log s$ of the square root of the average variance $F(s) = \sqrt{\frac{1}{n_s}\sum_{v=1}^{n_s} F^2(s,v)}$.

II. *MFDFA* The basic DFA technique is extended over the qth statistical moment of the calculated variance in terms of the scaling function (Mukli et al., 2015)

$$G(q,s) = \begin{cases} \left(\frac{1}{n_s}\sum_{v=1}^{n_s}[F^2(s,v)]^{\frac{q}{2}}\right)^{\frac{1}{q}}, & q \neq 0, \\ \exp\left(\frac{1}{n_s}\sum_{v=1}^{n_s}\ln\left[F^2(s,v)\right]\right), & q = 0. \end{cases} \tag{3}$$

The next step consists of calculation the q-order generalized Hurst exponent $H(q)$ from double logarithmic dependence $G(q,s) \sim s^{H(q)}$.
For the modified FB-MFDFA algorithm, the whole family of linear functions are fitted to the log–log dependence with the iterative optimization algorithm, see Wawrzkiewicz-Jałowiecka et al. (2020b) for details. It is worth to emphasize here that $H = H(q = 2)$ is the value of the Hurst exponent which is frequently used as a criterion for evaluation of a given series in terms of its predictability.
$H(q)$ is required to compute the next function — the singularity spectrum. In that aim, the mass exponent τ is estimated via the formula $\tau(q) = qH(q) - 1$. Next, the q-order Hölder exponent $h(q)$, is calculated, $h(q) = \frac{d\tau(q)}{dq}$. Finally, the q-order multifractal singularity spectrum $D(h)$ (mf-spectrum) is estimated as a Legendre transform of the mass exponent

$$D(h) = qh(q) - \tau(q) = q[h(q) - H(q)] + 1. \tag{4}$$

2.7. Multiscale entropy

I. *Sample Entropy estimation*
The Sample Entropy ($SampEn$) (Richman and Randall Moorman, 2000) represents the updated version of described by Pincus in 1991 Approximate Entropy ($ApEn$) (Pincus, 1991). The algorithm of Sample Entropy starts with a prior indication of two parameters: (i) the embedding dimension m which characterizes the length of vectors to compare, and (ii) the tolerance threshold r which is a criterion of similarity between two compared template vectors (usually selected between 10% and 20% of the calculated standard deviation of the time series amplitudes). For the calculations presented in this work the parameters $m = 2$ and $r = 0.15$ were used (Pincus, 1991).
The brief description of the ($SampEn$) method is presented below. At the first step a set of vectors $U_m(i)$, that represent m consecutive values of series $\{x_i\}_{i=1}^N$ is estimated.

$$U_m(i) = \{x_i, x_{i+1}, \ldots, x_{i+m-1}\}, \quad 1 \le i \le N - m + 1 \tag{5}$$

Next the distance between the $U_m(i)$ and $U_m(j)$ is calculated in the Euclidean form:

$$d[U_m(i), U_m(j)] = \max_{k=0,\ldots,m-1}(|x(i+k) - x(j+k)|) \tag{6}$$

In the further step the probability $C_i^m(r)$ that any $U_m(i)$ vector is matching to $U_m(j)$ is estimated. The $n_i^m(r)$ stands for a number of $U_m(j)$ vectors ($1 \le j \le N - m$, $j \neq i$) which are within the range of accepted tolerance threshold r i.e. $d[U_m(i), U_m(j)] \le r$.

$$C_i^m(r) = \frac{n_i^m(r)}{N - m} \tag{7}$$

The $C_i^m(r)$ is averaged over all vectors patterns $U_m(i)$ in order to estimate the probability $C^m(r)$ that any two vectors are within the r of each other

$$C^m(r) = \frac{1}{N - m + 1}\sum_{i=1}^{N-m+1} C_i^m(r) \tag{8}$$

The Sample Entropy $SampEn$ is a negative logarithm of the conditional probability that two sequences similar for m points remain similar for the $m + 1$ points.

$$SampEn(m, r, N) = -\log\left[\frac{C^{m+1}(r)}{C^m(r)}\right] \tag{9}$$

II. *Multiscale Entropy* estimation
The first step of estimation of Multiscale Entropy (MSE) consists of resampling procedure which is referred to as coarse-graining. This is obtained through averaging the data points in each of the non-overlapping segments with the increasing length λ in order to estimate signals of different time scales (y_j^λ).

$$y_j^\lambda = \frac{1}{\lambda}\sum_{i=(j-1)\lambda+1}^{j\lambda} x_i, \quad 1 \le j \le \frac{N}{\lambda} \tag{10}$$

For each y_j^λ series the value of $SampEn$ is calculated as a function of λ and finally plotted in the form of MSE curves.

2.8. Statistical testing

In case of normal distributions of nonlinear characteristics calculated for the mitoBK channels from different cell types the statistical testing was performed by the use of the Shapiro–Wilk formula and the Analysis of Variance (ANOVA). When the probability distributions of the evaluated parameters was not normal, the significance of the recognized differences was calculated via non-parametric Kruskal–Wallis test. In that case, the Mann–Whitney U statistic was used for the comparison of the nonlinear characteristics calculated for different cell lines. The selected significance level was $\alpha = 0.05$.

3. Theory

3.1. The utility of the MFDFA in investigations of gating dynamics

The multifractal detrended fluctuation analysis (MFDFA) is a tool used to describe the regularity of the occurrence of the fluctuations of different strengths. The MFDFA relies on the assumption that the signal is influenced by both short-term and long-term features, and consequently, also characterizes irregularity of experimental data over the range of time scales (Chhabra and Jensen, 1989; Makowiec and Fuliński, 2010; Ihlen, 2012; Mukli et al., 2015; Trybek et al., 2018a). This kind of analysis allows to obtain a set of spectral parameters that can be interpreted in terms of complexity of channel gating machinery. The first of these parameters is the Hurst exponent. In general, the Hurst analysis allows to characterize long-range correlations within a given time series (Hurst, 1951, 1965). The classical algorithm of its evaluation (Hurst, 1951, 1965) is applicable only to stationary time series while most physiological processes are nonstationary (statistical characteristics change with time). Thus, here we use the procedures of the DFA analysis (which extends the original Hurst approach) (Kantelhardt et al., 2002) The DFA technique (as well as its multifractal extension MFDFA) considers fluctuations around the trend. In consequence, it is more adequate to the data revealing non-stationary character which is a common feature of biological signals (Kristoufek, 2009). Some

advantages of detrended fluctuation analysis in applications to estimate long-range correlations within the signals can be found in the literature (Weron, 2002; Kirichenko et al., 2011). As mentioned before, the Hurst exponent H serves as the classification criterion in terms of the long-range memory effect (predictability). A Hurst exponent of 0.5 indicates purely uncorrelated random behavior of the considered system. If $0 < H < 0.5$, the system can be described as anti-persistent, where the increments of the adjacent elements of a given time series tend to switch between positive and negative values. The values of the Hurst exponent ranging over 0.5 suggest that the analyzed time series exhibits a long-term memory i.e. a trend-reinforcing behavior. In that case a positive increment of adjacent elements will tend to be followed by a positive one, and a negative increment will tend to be followed by a negative one. The larger the value of the Hurst exponent, the stronger the trend, and thus, it is easier to predict the future behavior of the system. The literature suggests that the long-range memory effect is a common feature of experimental data describing single channel activity both at the level of ionic current trace (Wawrzkiewicz-Jałowiecka et al., 2020b) and the series of dwell-times of subsequent channel states (Varanda et al., 2000; De Oliveira et al., 2006; Miśkiewicz et al., 2020; Borys, 2020; Wawrzkiewicz et al., 2012; Bahramian et al., 2019).

In this work, much emphasis is put on self-similar features of the system expressed by the power-law scaling of a "scaling function" (describing statistical moments of the signal's fluctuations) vs. window length (determined by actual time scale resolution). A central point of the analysis is a construction of a singularity spectrum based on the scaling function. The key parameters of the singularity spectra (e.g. spectral width Δ, symmetry of the spectrum) obtained for the experimental signal can be interpreted in terms of complexity and multifractality. The larger the Δ the more complex and richer the dynamics of a given system and the more evident a multifractal character of the analyzed series. Considering symmetry of a spectrum, presence of the left or right tail of a spectrum suggests insensitivity of the analyzed time series to the local fluctuations with small or large magnitudes, respectively. The multifractal and thermodynamic characteristics form a strong analogy. Namely, multifractal spectra can be related to system's entropy given by the Boltzmann's definition, which refers to the attainable substates of a system (stable conformations in the case of ion channel dynamics).

As in the case of other measures in the information theory, the multifractal methodology has gained a wide range of applications. The electrophysiological data or the medical image analysis are the main subject of research in this area (Gierałtowski et al., 2012; Makowiec et al., 2011; Trybek et al., 2018a; Braverman and Tambasco, 2013). There is only a small amount of work which deals with the multifractal characteristic of ion channel dynamics, narrowing the problem primarily to the potassium channels. Kazachenko et al. implemented MFDFA methodology for investigation of dwell time series of Ca^{2+}-activated K^+ channels in cultured kidney Vero cells. The same author proposed multifractal analysis of alamethicin channel kinetics (Kazachenko et al., 2007; Astashev et al., 2007). The multifractal nature of generated potassium ion current series was also demonstrated by Makowiec and Fuliński (2010).

3.2. The utility of the MSE analysis in investigations of gating dynamics

The multiscale entropy analysis (MSE) predicts the level of complexity by calculating how representative subseries are repetitive throughout the whole signal for a variety of time scales (Costa et al., 2002, 2005). The more repetitive are the recognized patterns within the signal, and as a consequence, the more regular is the analyzed series of data, the lower the value of sample entropy (SE) calculated at a given time scale. Additionally, a key point during this kind of analysis is the observation that both the signals exhibiting a perfect regularity as well as those showing complete randomness are not really complex. The MSE analysis incorporates the interrelationship of sample entropy and scale. In the case of a white noise, i.e. uncorrelated stochastic process of constant power spectrum, the entropy significantly monotonically decreases with the time scale. It is a consequence of the fact that as the time resolution decreases the average value inside each window (time interval determined by the actual time scale) converges to a fixed value. Thus, no new signal structures are revealed (Costa et al., 2005). The MSE allows to effectively describe complexity of a signal generated by an investigated biosystem, compare and discriminate its output from simple patterns stemming from either a regular deterministic control mechanism or fully uncorrelated white noise-like stochastic machinery.

From a macroscopic point of view, the MSE methodology is widely used in the biological context, especially for the distinction of health from pathology or identifying individual medical conditions. The most common in this area is the analysis of electrophysiological signals, including electrocardiography, electroencephalography and electromyography (Dharmaprani et al., 2018; Jun and Qian-Li, 2008; Trybek et al., 2018b; Miskovic et al., 2019; Angsuwatanakul et al., 2020). The thermodynamic aspect of entropy is considered much more often in case of analysis of gating dynamics (Sigg et al., 2003; Kim and Warshel, 2014; Wawrzkiewicz-Jałowiecka et al., 2017) than application of information theory. The notion of Shannon Entropy or Mutual Information were implemented to models of other phenomena referring to ion channels dynamics, e.g. stochastic resonance, which was described by Goychuk and Hänggi (2000). However, the reports about implementation of information entropy in this specific biological field i.e. studies on single-channel current data are lacking in the literature. One can only find a single report on application of multiscale entropy measures to assess the complexity of BK channels by performing the MSE analysis on the dwell-times sequences (Wawrzkiewicz-Jałowiecka et al., 2018). Considering the application and utility of the MSE analysis of experimental data describing the activity of ion channels, signal characteristics obtained by this method allow to describe the complexity of a switching mechanism between the substates of the channel microbiosystem (stable conformations). The higher values of multiscale entropy the more intricate mechanism should govern the conformational diffusion of the channel protein.

4. Results and discussion

4.1. mitoBK kinetics

Patch-clamp experiments performed with mitoplasts from human endothelium, fibroblasts and glioblastoma allow to uncover some differences in voltage activation within the investigated mitoBK channels, see Fig. 1 for details.

The sample traces of channel activity in Fig. 1a–c were selected as these parts of the patch-clamp recordings that can resemble the data characteristics of whole examined series.

In case of the EA.hy926 cell line, there was a small population of channels exhibiting a "lowered" gating where the p_{op} was low < 0.05 regardless of the applied voltage. This kind of behavior was probably caused by a typical inactivation of the BK channel conferred by $\beta 2$ subunits (Richard Benzinger et al., 2006; Wallner et al., 1999). Recordings representing lowered channel's activity were not taken to the further analysis, due to the fact that the main aim of this work is to analyze whether there exist some important differences in gating dynamics in a "normal" regime of mitoBK channels' activity. Inactivation is a kinetically distant process than gating.

As mentioned before, the functional heterogeneity caused by the presence of different β subunits associated with investigated channels as well as possibly alternative splicing of the Kcnma1 gene leading to multiple mitoBK channel isoforms significantly influence the voltage sensitivities, as presented in Fig. 1. The sigmoidal curve of p_{op} vs. U_m is shifted and shallower when one compares the activities of the mitoBK channels in endothelium, fibroblasts and astrocytoma. At the level of mean dwell-times of conducting and non-conducting states, the kinetics

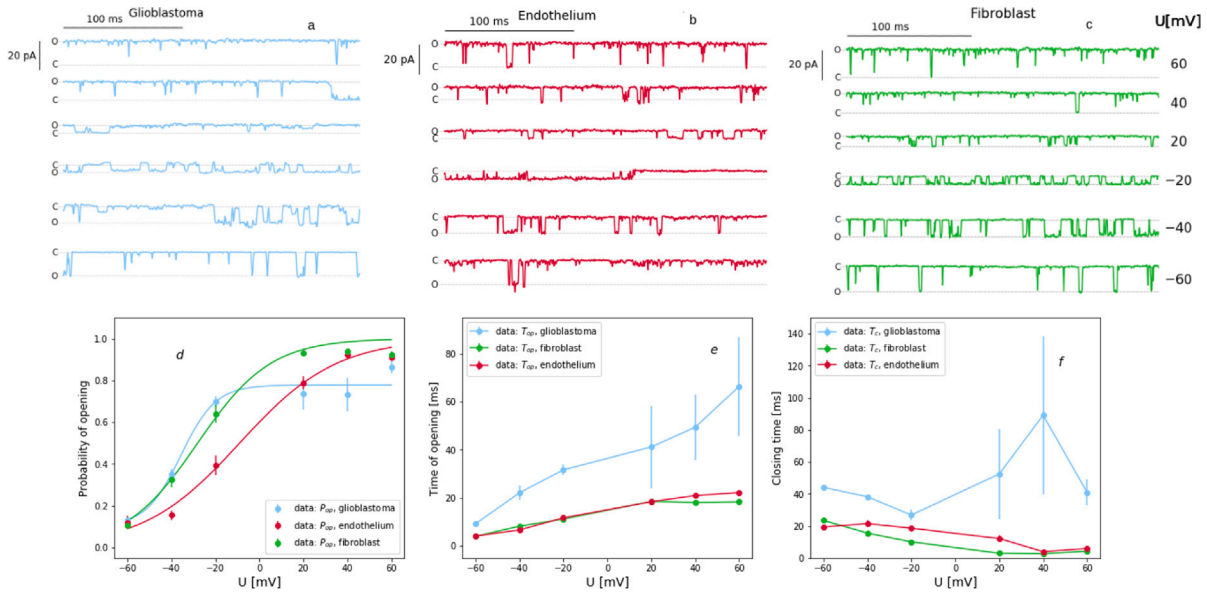

Fig. 1. The samples of the original signal of ionic current recorded from a single mitoBK channel over the range of membrane potential of three different cell types: glioblastoma (a); endothelium (b); fibroblast (c) and the average probability of channel opening (d); the average dwell-time of open state of the channel (e) and the average dwell-time of the functionally closed state of the channel (f) calculated for glioblastoma, fibroblasts and endothelium.

of mitochondrial BK channels assembled with $\beta 2$ and $\beta 3$ ought to share many similarities (as seen by p_{op}s, τ_{op}s and τ_{cl} corresponding to mitoBK channels from endothelium and fibroblasts). The kinetic properties of mitochondrial BK channels from astrocytoma (in complex with $\beta 4$ subunits) relevantly differ from the other ones. The mitoBK channels from glioblastoma are also most internally differentiated which is indicated by high values of the standard deviations presented as error bars in Fig. 1.

Considering the recognized kinetic diversity in the channel gating from different cell lines, one can ponder whether this effect is additionally biased by differences in response to mechanical stimulation of the membrane during mitoplast-attached single channel mode of the performed experiments. To evaluate the effects of mechanical strain on the analyzed patches one should realize the following facts:

- It is well-known that the mechanical stimulation imposed by experimental procedure can influence the channel system to some extent, what was summarized e.g. by Sachs (2010) and Suchyna et al. (2009).
- The mechanosensitivity of the BK channels and the presence of a STREX exon in specific mitochondrial BK splice variants are reported in Refs. Wawrzkiewicz-Jałowiecka et al. (2018) and Walewska et al. (2018).
- Different distributions of the splice variants involved in channel's activation by mechanical strain in the analyzed cell types cannot be precluded.

Nevertheless, in the case of our studies the mechanical strains within the inner mitochondrial membrane are most evident at the stage of induction of osmotic shock (to impose swelling of mitochondria), but after gaining a gigaseal and excising the patch, only a resting tension in the patch dome remains. Then, no additional membrane suction is imposed. In that terms, the patch-clamp recordings are carried out.

Thus, we are convinced that there is no need to comment on any additional effects of mechanical stimulation of the membrane on channel gating in the considered case. Moreover, all the investigated patches are handled in the same way, so similar effects arising from the membrane condition affect channels' activities. Since in the current work we comment the relative characteristics of the mitoBK-β complexes (or different mitoBK isoform — β assemblies in the analyzed populations of channels), all inferences pertain to the dynamical diversity of the system arising mainly from different types of β subunits (and/or possibly different dominating channel's isoforms) and not from the mechanical or physicochemical factors which were comparable in all experimental configurations.

4.2. Complexity of mitoBK signal

4.2.1. MFDFA

The representative scaling functions (F_q) of each cell line are presented in Fig. 2. Within the length of the investigated data (50 000 data points for each series) we selected the range of scales $s \in [2^4, 2^9]$. In this range the linear trends of the double-logarithmic dependencies of F_q on scales are visible.

The first parameter obtained by the use of the MFDFA method (Kantelhardt et al., 2002) is the Hurst exponent and the obtained results are presented in Fig. 3. The long-range correlations in single mitoBK channel currents are preserved regardless of membrane potential, as well as the cell type. Moreover, the trend-reinforcing behavior seem to be a common feature of a channel gating regardless of where they are located: in cell membrane (Wawrzkiewicz-Jałowiecka et al., 2020b) or membranes within single organelle, as presented here in case of the inner mitochondrial membrane. Fig. 3 shows that in every investigated group of mitoBK channels there are no clear, monotonic, or repeatable tendencies in H vs. U_m plots. When comparing different cell types, one can observe that the highest values of the Hurst exponent are reached for glioblastoma (except for $U_m = -40$ mV). This relation determines the strength of long-range memory effects in time series of single-channel currents, which is, consequently, highest in case of the glioblastoma cells. What is a general observation (valid for all analyzed types of cells) it is that the Hurst exponent tends to take the higher values at membrane hyperpolarization than at its depolarization.

Considering the other spectral parameters, we have obtained considerably wide spectra during the multifractal analysis of all investigated data sets (Fig. 4). It indicates that the multiscale self-similarity of a signal can be considered as a common feature of single-mitoBK channel currents, which neither depends on the membrane potential nor the cell type, where a given channel is expressed. Although all time series have a multifractal characteristics, the values of spectral parameters (viz., spectral width Δ, half-width $\Delta_{1/2}$, maximum of a spectrum h_{max}, spectral

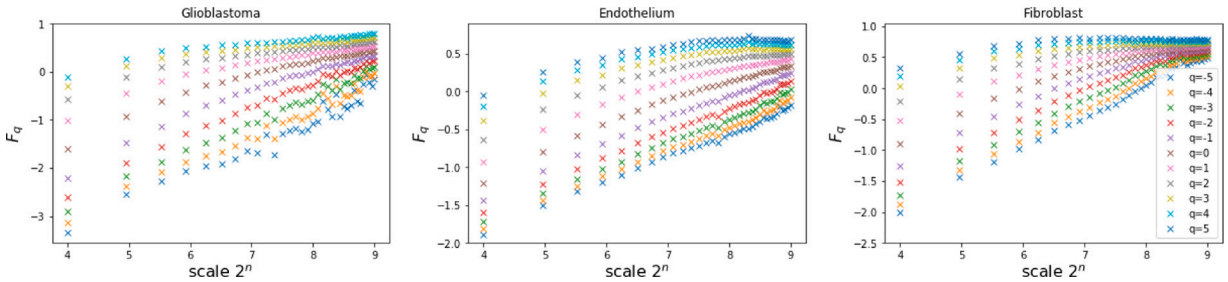

Fig. 2. The representative scaling function calculated for $s \in [2^4, 2^9]$ range of scales and $q \in [-5, 5]$ obtained for the mitoBK channels from different cell types at $U_m = -20$ mV.

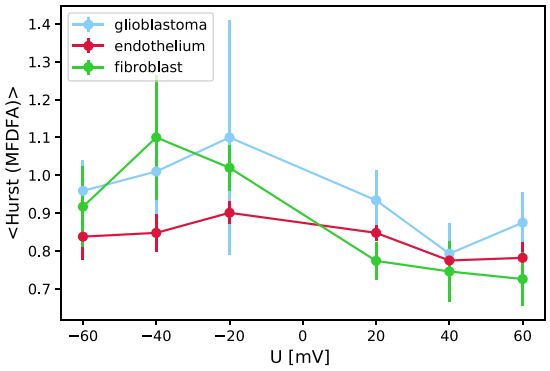

Fig. 3. The Hurst exponent calculated by the MFDFA method for the experimental series of single-channel currents obtained for three different cell types.

symmetry) allow to distinguish the analyzed groups of mitoBK channels from each other. The average multifractal spectra calculated for the series of ionic currents registered at different membrane potentials are presented in Fig. 4, whilst the parameters used for their description are presented in Fig. 5.

Multifractal spectra representing all mentioned data sets can be clearly discerned by the location of maximum (Fig. 4 left panel). The other parameters do not allow for a so clear distinguishment between the recordings of mitoBK activity in all analyzed cell types. Considering the spectrum width Δ, it turns out that the broadest spectrum represents the mitoBK-β4 complex in glioblastoma (which suggest the largest number of attainable channel's conformations, according to the definition of Boltzmann's entropy). The similar values of Δ in case of mitoBK channels from endothelium and fibroblasts indicate similar size of conformational spaces of mitoBK-β2 and mitoBK-β3 assemblies.

Considering the changes of spectral parameters with voltage (one can observe that all the time series representing mitoBK channels exhibit $\Delta(U_m)$ and $\Delta_{1/2}(U_m)$ dependencies with the minima located at moderate values of membrane potential (see Fig. 5 – panels b and c). This suggests that the number of available conformations should increase with the difference in electric potential across the membrane both for positive and negative voltages. This kind of $\Delta(U_m)$ and $\Delta_{1/2}(U_m)$ dependencies seem to be a common features of the BK channels, regardless from they are located in mitochondrial or cell membrane (Wawrzkiewicz-Jałowiecka et al., 2020b,a) or in different types of cells.

What is worth noticing is that for all the analyzed values of U_m the most evident asymmetry of the multifractal singularity spectra representing mitoBK channels in glioblastoma with the prominent long right-hand-side tails. This suggest that these time series have a multifractal structure which is insensitive to the local fluctuations with large magnitudes.

Considering the other spectral parameters, in the vast majority of cases the statistically significant differences were identified. There is only four exceptions, namely, there is no statistically significant differences between the values of calculated parameters at the different cell types in the following cases: Hurst exponent at the −60 mV (p = 0.068), h_{max} at the 40 mV (p = 0.083) $\Delta_{1/2}$ at the U_m levels of 20 mV and 60 mV (p = 0.208 and p = 0.264); the p values are obtained for the Kruskal–Wallis test.

4.2.2. Multiscale entropy

The results of multiscale entropy analysis calculated for ionic currents of the investigated mitoBK channels are presented in Fig. 6. It can be observed that in general, signal complexity increases with the time scale. The coarse graining of a time series of single-channel currents representing system behavior unravels new structures of a signal at large time scales. This effect is more evident at membrane hyperpolarization than at membrane depolarization. It suggests that at negative membrane potentials the signal is highly affected by the processes occurring at a larger time scale in relation to the conformational diffusion of a channel protein. The possible candidates for such processes are fluctuations in membrane thickness or membrane vibrations. In case of membrane depolarization, one can observe relatively fast stabilization of the SE vs. scale curve, which can be interpreted in terms of domination of short-lasting components in shaping the structure of recorded signal (these components result almost only from the activity of a channel). Another general observation that can be made from the obtained results is that higher values of the MSE are reached for membrane depolarization than at membrane hyperpolarization regardless of the cell type. One can infer that during membrane depolarization the complexity of the mechanism of switching between different channel substates increases, and consequently, the predictability of a system declines. At membrane hyperpolarization, when the channel tends to retain non-conducting states, conformational dynamics is realized in a more repetitive manner. Comparing the mitoBK channels from different cell types, it can be observed that the variability of the MSE with the U_m is the highest for fibroblasts and the lowest for glioblastoma. Thus, the dynamical changeability of switching between the substates in a conformational space of mitochondrial BK channels in complex with the β3 subunits is more evidently expressed in comparison with the other analyzed mitoBK-β assemblies.

As mentioned in the *Introduction* the decrease in complexity reflects loss in the ability of a given biosystem to adjust to an ever-changing environment and it is often caused by decoupling or degradation of a control mechanism as a consequence of possible existing pathology. This general feature is also expressed by the MSE results. The only pathological cell line used in this research is the glioblastoma U-87 MG. The inner mitochondrial BK channels in these cells can be distinguished from the other ones by the lower MSE values at membrane depolarization i.e. in terms when the channel should most effectively conduct ions to fulfill its biological role. This suggests that a pathology expressed at the level of a cell line finds its representation even at the level of a single channel protein functioning within an organelle.

The obtained results of multiscale entropy analysis are in good agreement with the results of the Hurst analysis according to the MFDFA algorithm, provided in the former subsection. In general, the more evident is a long-term memory effect (as measured by high values

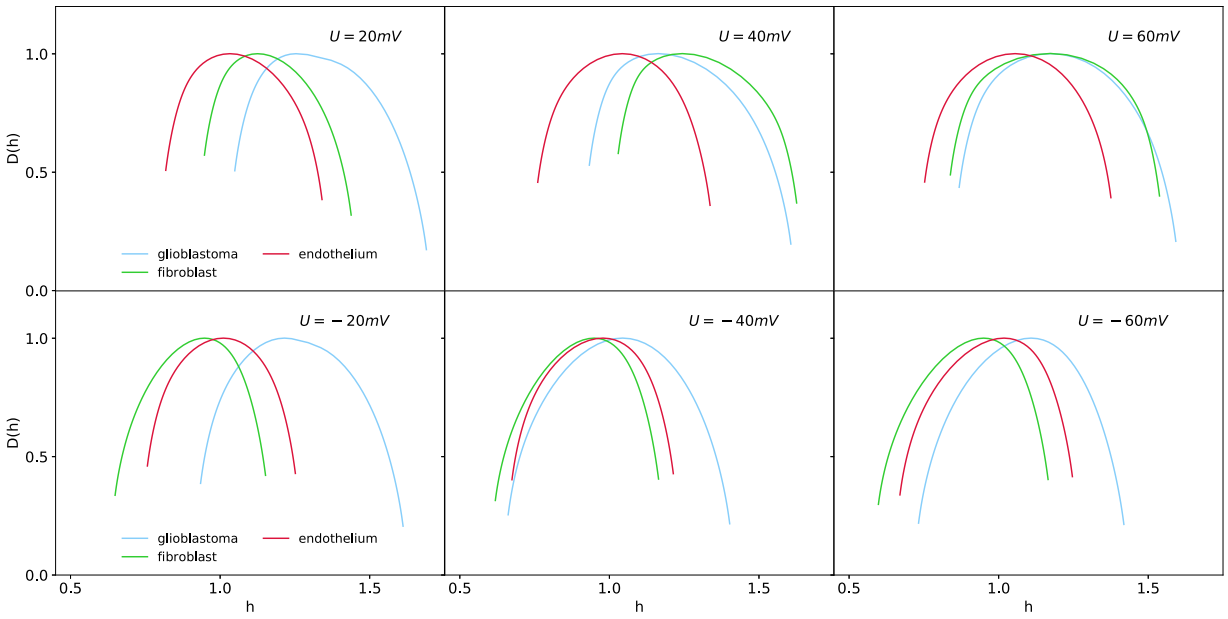

Fig. 4. Comparison of multifractal spectra corresponding to single-mitoBK channel currents from different cell types.

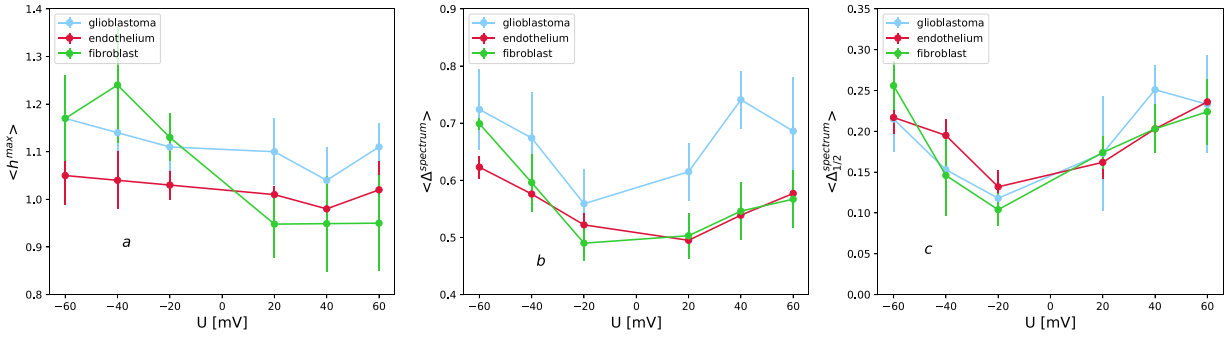

Fig. 5. The parameters of multifractal spectra: maximum of spectrum (a), spectrum width (b), spectrum half-width (c) for the mitoBK channels from different cell types.

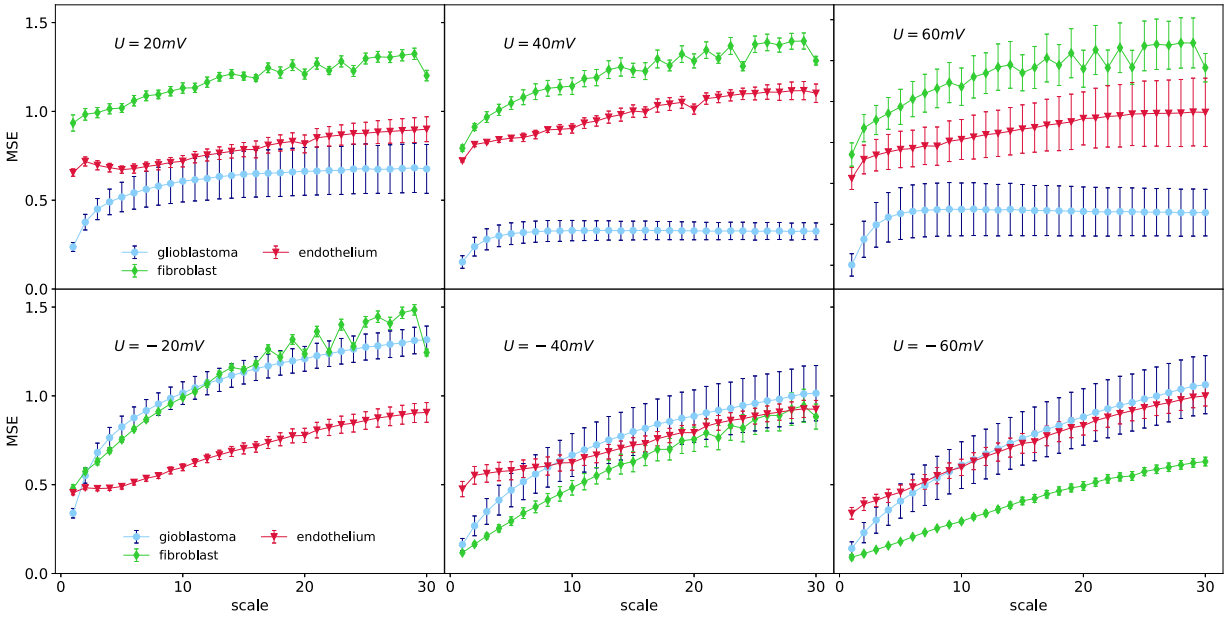

Fig. 6. Multiscale entropy calculated for the single-channel currents representing the mitoBK channels from three different cell types: glioblastoma (blue), fibroblasts (green) and endothelium (red).

of the Hurst exponent), the more predictable the series, and the lower are the values of the MSE. It is particularly evident at positive values of membrane potential, where the Hurst exponent reaches the highest values for glioblastoma, medium ones — for endothelium and the lowest for fibroblasts. The MSE raises in the opposite order.

Due to the lack of normal probability distributions of the MSE the significance of the recognized differences was calculated via non-parametric Kruskal–Wallis test and Mann–Whitney U statistic, respectively. All considered cases indicate statistically significant differences between $SampEn$ values calculated over the whole range of scales ($p < 0.05$).

5. Conclusions

The nonlinear methods of analysis allow to indicate dynamical diversity among the mitochondrial BK channels located in different cell types. The recognized differences are associated mainly with the tissue-specific occurrence of different β subunits co-assembled to the channel. Even in case of the channels in a complex with $\beta 2$ subunits (from endothelial cells) and $\beta 3$ subunits (from fibroblasts), which have very similar kinetic characteristics, the MSE and MFDFA methods allowed to find individual features of these two groups, that enable for discerning them from each other. In general, differences in dominating type of mitoBK α-β assembly can influence the structural richness, tendency to exhibit repeatable sequences, trend-reinforcing behavior or multifractal features within biological signals representing a single-channel activity.

The nonlinear methods of analysis can provide a useful tool in investigation of conformational dynamics of a channel protein and development of kinetic models of channel activation and gating. In particular, the multiscale entropy analysis allow us to describe the complexity of switching mechanism between the available channel conformations at given external conditions. The multifractal detrended fluctuation analysis enable us to determine relative numbers of the attainable substates of a channel. Thus, the spectral parameters can be used to uncover the main tendencies in the changes of effectively attainable channel conformations while acting of an activating stimulus (e.g. membrane depolarization). Our results allowed us to infer that the mitoBK from glioblastoma cells channels may be able to fluctuate between a larger number of available channel conformations than their counterparts from the other cell lines. However, the way of switching between the stable conformations is realized in a more repetitive way in case of mitoBK channels from glioblastoma in comparison with the other cell types (as indicated by the results of the MSE analysis).

Referring to the most important results provided in this work, one has to mention the significant loss in biological signal's complexity in the case of single mitoBK channel current from glioblastoma, as shown by the MSE analysis at intermediate and high values of membrane potentials in Fig. 6. A decrease of complexity may be a generic feature of pathological dynamics (Costa et al., 2005), thus the lowest multiscale entropy of ionic currents through the mitoBK channels from astrocytoma in comparison with analogous data describing the channels' activity in other cell types seem to agree with this rule. Moreover, the studies of the BK channels located in cellular membrane in glioma cells (Ransom et al., 2002; Weaver et al., 2006) suggest that these channels are expressed in specific isoforms that have slightly different characteristics from other BK channel exons (e.g., they are more sensitive to cytosolic concentration of Ca^{2+}). Our results of kinetic, Hurst, MSE and MFDFA analyses confirmed different physiological features of the BK channels in glioblastoma cells from the channels expressed in other cell lines. This distinction can be seen also at the level of mitochondria.

Application of the MFDFA analysis to patch-clamp traces of mitoBK channel activity allowed for the inference that, probably, $\beta 2$ and $\beta 3$ subunits assembled to the channel do not create new channel conformations at high and moderate values of membrane potential and they exert only a minor effect on the preexisting set of channel conformations at deep hyperpolarization ($U_m = -60$ mV) of a membrane (Figs. 1, 5 – middle panel). However, these auxiliary subunits ought to change the scheme of switching between the preexisting conformations of a channel pore, as shown by the differences in the results of the MSE for different cell types (Fig. 6).

Considering a possible applications of the methods of analysis presented here, one can list the artificial intelligence (AI) approaches (e.g., deep learning, neural networks) which can be used for diagnosing, managing, and designing drugs against many popular diseases (Amato et al., 2013; Hessler and Baringhaus, 2018; Jordan, 2018; Mak and Pichika, 2019). Machine learning techniques can be developed where some of the classification algorithms will be based on the results of the MFDFA and MSE analyses in the aim to examine patterns within the experimental data describing ion-channel activity with or without the use of specific channel modulators. Such an approach may simplify the choice of the most effective activating/inhibiting substances. Thus, the results obtained here can provide a theoretical background for further investigations on the potential modulators of the mitochondrial BK channels (like e.g. natural flavonoids).

CRediT authorship contribution statement

Agata Wawrzkiewicz-Jałowiecka: Conceptualization of this study, Methodology, Software, Writing - Original draft, Supervision, Validation, Visualization, Writing review & editing, Project administration. **Paulina Trybek:** Conceptualization of this study, Methodology, Software, Writing - original draft preparation, Statistical analysis, Visualization. **Łukasz Machura:** Software, Methodology, Writing - original draft, Writing review & editing. **Piotr Bednarczyk:** Data curation, Writing - original draft, Validation, Writing review & editing, Project administration.

Declaration of competing interest

The authors declare that they have no known competing financial interests or personal relationships that could have appeared to influence the work reported in this paper.

Acknowledgments

Agata Wawrzkiewicz-Jałowiecka was supported by the Silesian University of Technology, Poland Grant for young researchers BKM-528/RCh4/2020 (statute project). This study was also supported by grant 2016/21/B/NZ1/02769 and 2019/35/B/NZ1/02546 both from the National Science Center of Poland (to PB). Partially experimental data were obtained at Nencki Institute of Experimental Biology, Warsaw, Poland and Otto-von-Guericke-University, Magdeburg, Germany.

References

Amato, Filippo, López, Alberto, Peña-Méndez, Eladia María, Vaňhara, Petr, Hampl, Aleš, Havel, Josef, 2013. Artificial Neural Networks in Medical Diagnosis. Elsevier.

Angsuwatanakul, Thanate, O'Reilly, Jamie, Ounjai, Kajornvut, Kaewkamnerdpong, Boonserm, Iramina, Keiji, 2020. Multiscale entropy as a new feature for eeg and fnirs analysis. Entropy 22 (2), 189.

Astashev, M.E., Kazachenko, V.N., Grigoriev, P.A., 2007. Alamethicin channel kinetics: Studies using fluctuation analysis and multifractal fluctuation analysis. Biochem. (Moscow) Suppl. Ser. A 1 (3), 246–252.

Bahramian, Alireza, Nouri, Ali, Baghdadi, Golnaz, Gharibzadeh, Shahriar, Towhidkhah, Farzad, Jafari, Sajad, 2019. Introducing a chaotic map with a wide range of long-term memory as a model of patch-clamped ion channels current time series. Chaos Solitons Fractals 126, 361–368.

Balderas, Enrique, Torres, Natalia S., Rosa-Garrido, Manuel, Chaudhuri, Dipayan, Toro, Ligia, Stefani, Enrico, Olcese, Riccardo, 2019. Mitobkca channel is functionally associated with its regulatory $\beta 1$ subunit in cardiac mitochondria. J. Physiol. 597 (15), 3817–3832.

Balderas, Enrique, Zhang, Jin, Stefani, Enrico, Toro, Ligia, 2015. Mitochondrial bkca channel. Front. Physiol. 6, 104.

Bednarczyk, Piotr, Koziel, Agnieszka, Jarmuszkiewicz, Wieslawa, Szewczyk, Adam, 2013a. Large-conductance ca2+-activated potassium channel in mitochondria of endothelial ea. hy926 cells. Amer. J. Physiol.-Heart Circ. Physiol. 304 (11), H1415–H1427.

Bednarczyk, Piotr, Wieckowski, Mariusz R, Broszkiewicz, Malgorzata, Skowronek, Krzysztof, Siemen, Detlef, Szewczyk, Adam, 2013b. Putative structural and functional coupling of the mitochondrial bkca channel to the respiratory chain. PLoS One 8 (6).

Borys, Przemyslaw, 2020. Long term hurst memory that does not die at long observation times—Deterministic map to describe ion channel activity. Chaos Solitons Fractals 132, 109560.

Braverman, Boris, Tambasco, Mauro, 2013. Scale-specific multifractal medical image analysis. Comput. Math. Methods Med. 2013.

Chhabra, Ashvin, Jensen, Roderick V., 1989. Direct determination of the f (α) singularity spectrum. Phys. Rev. Lett. 62 (12), 1327.

Contreras, Gustavo F., Neely, Alan, Alvarez, Osvaldo, Gonzalez, Carlos, Latorre, Ramon, 2012. Modulation of bk channel voltage gating by different auxiliary β subunits. Proc. Natl. Acad. Sci. 109 (46), 18991–18996.

Costa, Madalena, Goldberger, Ary L., Peng, C.-K., 2002. Multiscale entropy analysis of complex physiologic time series. Phys. Rev. Lett. 89 (6), 068102.

Costa, Madalena, Goldberger, Ary L., Peng, C.-K., 2005. Multiscale entropy analysis of biological signals. Phys. Rev. E 71 (2), 021906.

De Oliveira, R.A. Campos, Barbosa, C.T.F., Consoni, L.H.A., Rodrigues, A.R.A., Varanda, Wamberto Antônio, Nogueira, R.A., 2006. Long-term correlation in single calcium-activated potassium channel kinetics. Physica A 364, 13–22.

Dharmaprani, Dhani, Dykes, Lukah, McGavigan, Andrew D., Kuklik, Pawel, Pope, Kenneth, Ganesan, Anand N., 2018. Information theory and atrial fibrillation (af): A review. Front. Physiol. 9, 957.

Duchen, Michael R., 2000. Mitochondria and calcium: from cell signalling to cell death. J. Physiol. 529 (1), 57–68.

Gierałtowski, J., Żebrowski, J.J., Baranowski, R., 2012. Multiscale multifractal analysis of heart rate variability recordings with a large number of occurrences of arrhythmia. Phys. Rev. E 85 (2), 021915.

Goychuk, Igor, Hänggi, Peter, 2000. Stochastic resonance in ion channels characterized by information theory. Phys. Rev. E 61 (4), 4272.

Halestrap, Andrew P., 1994. Regulation of Mitochondrial Metabolism through Changes in Matrix Volume. Portland Press Ltd..

Hessler, Gerhard, Baringhaus, Karl-Heinz, 2018. Artificial intelligence in drug design. Molecules 23 (10), 2520.

Hurst, Harold Edwin, 1951. Long-term storage capacity of reservoirs. Trans. Amer. Soc. Civ. Eng. 116, 770–799.

Hurst, Harold Edwin, 1965. Long term storage. Exp. Study.

Ihlen, Espen Alexander Fürst E.A.F.I, 2012. Introduction to multifractal detrended fluctuation analysis in matlab. Front. Physiol. 3, 141.

Jordan, Allan M., 2018. Artificial Intelligence in Drug Design—the Storm Before the Calm? ACS Publications.

Jun, Wang, Qian-Li, Ma, 2008. Multiscale entropy based study of the pathological time series. Chin. Phys. B 17 (12), 4424.

Kantelhardt, Jan W., Zschiegner, Stephan A., Koscielny-Bunde, Eva, Havlin, Shlomo, Bunde, Armin, Eugene Stanley, H., 2002. Multifractal detrended fluctuation analysis of nonstationary time series. Physica A 316 (1–4), 87–114.

Kazachenko, V.N., Astashev, M.E., Grinevich, A.A., 2007. Multifractal analysis of k+ channel activity. Biochem. (Moscow) Suppl. Ser. A 1 (2), 169–175.

Kicinska, Anna, Augustynek, Bartlomiej, Kulawiak, Bogusz, Jarmuszkiewicz, Wieslawa, Szewczyk, Adam, Bednarczyk, Piotr, 2016. A large-conductance calcium-regulated k+ channel in human dermal fibroblast mitochondria. Biochem. J. 473 (23), 4457–4471.

Kim, Ilsoo, Warshel, Arieh, 2014. Coarse-grained simulations of the gating current in the voltage-activated kv1. 2 channel. Proc. Natl. Acad. Sci. 111 (6), 2128–2133.

Kirichenko, Ludmila, Radivilova, Tamara, Deineko, Zhanna, 2011. Comparative analysis for estimating of the hurst exponent for stationary and nonstationary time series. Inf. Technol. Knowl. 5 (1), 371–388.

Kowaltowski, Alicia J., de Souza-Pinto, Nadja C., Castilho, Roger F., Vercesi, Anibal E., 2009. Mitochondria and reactive oxygen species. Free Radic. Biol. Med. 47 (4), 333–343.

Kristoufek, Ladislav, 2009. R/s analysis and dfa: finite sample properties and confidence intervals. MPRA.

Mak, Kit-Kay, Pichika, Mallikarjuna Rao, 2019. Artificial intelligence in drug development: present status and future prospects. Drug Discov. Today 24 (3), 773–780.

Makowiec, Danuta, Fuliński, Andrzej, 2010. Multifractal detrended fluctuation analysis as the estimator of long-range dependence. Acta Phys. Polon. B 41 (5).

Makowiec, Danuta, Rynkiewicz, Aleksandra, Gałaska, R., Wdowczyk-Szulc, J., Żarczyńska-Buchowiecka, M., 2011. Reading multifractal spectra: aging by multifractal analysis of heart rate. Europhys. Lett. 94 (6), 68005.

Mercik, Szymon, Weron, Karina, Siwy, Zuzanna, 1999. Statistical analysis of ionic current fluctuations in membrane channels. Phys. Rev. E 60 (6), 7343.

Miśkiewicz, Janusz, Trela, Zenon, Burdach, Zbigniew, Karcz, Waldemar, Balińska-Miśkiewicz, Wanda, 2020. Long range correlations of the ion current in sv channels. Met3pbcl influence study. PLoS One 15 (3), e0229433.

Miskovic, Vladimir, MacDonald, Kevin J., Jack Rhodes, L., Cote, Kimberly A., 2019. Changes in eeg multiscale entropy and power-law frequency scaling during the human sleep cycle. Human Brain Mapp. 40 (2), 538–551.

Mukli, Peter, Nagy, Zoltan, Eke, Andras, 2015. Multifractal formalism by enforcing the universal behavior of scaling functions. Physica A 417, 150–167.

Papadopoulos, Vassilios, Miller, Walter L., 2012. Role of mitochondria in steroidogenesis. Best Pract. Res. Clin. Endocrinol. Metab. 26 (6), 771–790.

Peng, C.-K., Buldyrev, Sergey V., Havlin, Shlomo, Simons, Michael, Eugene Stanley, H., Goldberger, Ary L., 1994. Mosaic organization of dna nucleotides. Phys. Rev. E 49 (2), 1685.

Pincus, S.M., 1991. Approximate entropy: a complexity measure for biological time series data. In: Proceedings of the 1991 IEEE Seventeenth Annual Northeast Bioengineering Conference. pp. 35–36.

Pincus, Steven M., 1991. Approximate entropy as a measure of system complexity. Proc. Natl. Acad. Sci. 88 (6), 2297–2301.

Piwonska, M., Wilczek, E., Szewczyk, A., Wilczynski, G.M., 2008. Differential distribution of ca2+-activated potassium channel β4 subunit in rat brain: immunolocalization in neuronal mitochondria. Neuroscience 153 (2), 446–460.

Ransom, Christopher B., Liu, Xiaojin, Sontheimer, Harald, 2002. Bk channels in human glioma cells have enhanced calcium sensitivity. Glia 38 (4), 281–291.

Richard Benzinger, G., Xia, Xiao-Ming, Lingle, Christopher J., 2006. Direct observation of a preinactivated, open state in bk channels with β2 subunits. J. Gen. Physiol. 127 (2), 119–131.

Richman, Joshua S., Randall Moorman, J., 2000. Physiological time-series analysis using approximate entropy and sample entropy. Amer. J. Physiol.-Heart Circ. Physiol. 278 (6), H2039–H2049.

Sachs, Frederick, 2010. Stretch-activated ion channels: what are they? Physiology 25 (1), 50–56.

Sigg, Daniel, Bezanilla, Francisco, Stefani, Enrico, 2003. Fast gating in the shaker k+ channel and the energy landscape of activation. Proc. Natl. Acad. Sci. 100 (13), 7611–7615.

Singh, Harpreet, Lu, Rong, Bopassa, Jean C., Meredith, Andrea L., Stefani, Enrico, Toro, Ligia, 2013. Mitobkca is encoded by the kcnma1 gene, and a splicing sequence defines its mitochondrial location. Proc. Natl. Acad. Sci. 110 (26), 10836–10841.

Suchyna, Thomas M., Markin, Vladislav S., Sachs, Frederick, 2009. Biophysics and structure of the patch and the gigaseal. Biophys. J. 97 (3), 738–747.

Szabo, Ildiko, Zoratti, Mario, 2014. Mitochondrial channels: ion fluxes and more. Physiol. Rev. 94 (2), 519–608.

Tao, Xiao, MacKinnon, Roderick, 2019. Molecular structures of the human slo1 k+ channel in complex with β4. eLife 8.

Trybek, Paulina, Nowakowski, Michal, Machura, Lukasz, 2018a. Multifractal characteristics of external anal sphincter based on semg signals. Med. Eng. Phys. 55, 9–15.

Trybek, Paulina, Nowakowski, Michal, Salowka, Jerzy, Spiechowicz, Jakub, Machura, Lukasz, 2018b. Sample entropy of semg signals at different stages of rectal cancer treatment. Entropy 20 (11), 863.

Varanda, Wamberto A., Liebovitch, Larry S., Figueiroa, Jose N., Nogueira, Romildo A., 2000. Hurst analysis applied to the study of single calcium-activated potassium channel kinetics. J. Theoret. Biol. 206 (3), 343–353.

Walewska, Agnieszka, Kulawiak, Bogusz, Szewczyk, Adam, Koprowski, Piotr, 2018. Mechanosensitivity of mitochondrial large-conductance calcium-activated potassium channels. Biochim. Biophys. Acta (BBA)-Bioenerg. 1859 (9), 797–805.

Wallner, Martin, Meera, Pratap, Toro, Ligia, 1999. Molecular basis of fast inactivation in voltage and ca2+-activated k+ channels: a transmembrane β-subunit homolog. Proc. Natl. Acad. Sci. 96 (7), 4137–4142.

Wang, Xiaodong, 2001. The expanding role of mitochondria in apoptosis. Genes Dev. 15 (22), 2922–2933.

Wawrzkiewicz, Agata, Pawelek, Krzysztof, Borys, Przemyslaw, Dworakowska, Beata, Grzywna, Zbigniew J., 2012. On the simple random-walk models of ion-channel gate dynamics reflecting long-term memory. Eur. Biophys. J. 41 (6), 505–526.

Wawrzkiewicz-Jałowiecka, Agata, Dworakowska, Beata, Grzywna, Zbigniew J., 2017. The temperature dependence of the bk channel activity–kinetics, thermodynamics, and long-range correlations. Biochim. Biophys. Acta (BBA)-Biomembr. 1859 (10), 1805–1814.

Wawrzkiewicz-Jałowiecka, Agata, Trybek, Paulina, Borys, Przemysław, Dworakowska, Beata, Machura, Łukasz, Bednarczyk, Piotr, 2020a. Differences in gating dynamics of bk channels in cellular and mitochondrial membranes from human glioblastoma cells unraveled by short-and long-range correlations analysis. Cells 9 (10), 2305.

Wawrzkiewicz-Jałowiecka, Agata, Trybek, Paulina, Dworakowska, Beata, Machura, Łukasz, 2020b. Multifractal properties of bk channels' currents in human glioblastoma cells. J. Phys. Chem. B.

Wawrzkiewicz-Jałowiecka, Agata, Trybek, Paulina, Machura, Łukasz, Dworakowska, Beata, Grzywna, Zbigniew J., 2018. Mechanosensitivity of the bk channels in human glioblastoma cells: Kinetics and dynamical complexity. J. Membr. Biol. 251 (5–6), 667–679.

Weaver, Amy K., Bomben, Valerie C., Sontheimer, Harald, 2006. Expression and function of calcium-activated potassium channels in human glioma cells. Glia 54 (3), 223–233.

Weron, Rafał, 2002. Estimating long-range dependence: finite sample properties and confidence intervals. Physica A 312 (1–2), 285–299.